

Automatic Estimation of Defects in Composite Structures as Disturbances Based on Machine Learning Classifiers Oriented Mathematical Models with Uncertainties

A. A. Zhilenkov¹, S. G. Chernyi^{1,2,3}

¹ St. Petersburg State Marine Technical University, St. Petersburg, Russia

² Admiral Makarov State University of Maritime and Inland Shipping, St. Petersburg, Russia

³ Kerch State Maritime Technological University, Kerch, Russia

Abstract: The proposed system for detecting defects in composite materials, such as carbon fiber or textile fabric, is described. Defects in the structure of the product are detected using a computer vision system based on optical sensors, i.e. a visual inspection is carried out - a necessary stage in the production process of composite materials. The difference of the proposed method from the existing solutions is the unique model of the sensor-material interaction and its strict mathematical description. A comparison with the reference model of the structure specified analytically is used.

Keywords: mathematical modeling; flaw detection; inspection; sensors; composites; machine learning

DOI 10.14357/20718632200302

Introduction

The object of inspection, which is considered in this study, is the fabric formed by the mutual interweaving of the threads of two systems located in two mutually perpendicular directions from each other. The threads of one system that go along the fabric are called the warp, and the threads of the other system that go across the fabric - the weft. In the production of fabrics, it is necessary that the warp threads have their own constant tension created by a special mechanism. The value of the tension varies cyclically, which leads to multiple stretching of the warp threads. Modern production plants have a complex, highly developed technological base, which provides flexibility of control and optimization of the parameters of technological process when changing the properties of raw

materials. Technological processes for the production of composite materials and textile fabrics are complex and interconnected, which is explained by the properties of the materials being treated and the methods for their treating [1-5].

Let's review on the prior techniques and models, which researchers have been using for fabric defect detection. In statistical approaches there are defect detection methods using: fractal dimension, bi-level thresholding, gray level statistics, morphological operations, edge detection, normalized cross-correlation, co-occurrence matrix features, eigenfilters, local linear transforms, rank-order functions, neural-networks. These methods are based on very high-dimensional statistics. Thus, they are very consuming in terms of processing time and memory. Another problem with them is inefficiency when there is several defects at the

same time. As for methods based on classification, large number of fabric defect classes with large intra-class diversity remain major obstacles in using such systems as feed-forward networks [5, 11] and support vector machine [11] for online fabric inspection.

In spectral approaches there are defect detection methods using: discrete Fourier transform, optical Fourier transform, windowed Fourier transform, Gabor filters, Optimized FIR filters, Wigner distributions, wavelet transform. In general, such approaches [3, 4] cannot detect defects that appear as subtle change in fabric texture.

In model-based approaches there are defect detection methods using: Gauss Markov Random Field model, Poisson's model, model-based clustering. So, there is not many model-based approaches, and existing ones are based on stochastic models. The performance of these methods is not satisfactory when there is gray colors dominate in the image [18].

On one side, mentioned methods are computationally expensive and require much tuning. On another, inspection of patterned webs has remained largely unexplored and most of attempts [15-18] to deal with this problem have focused on mechatronics approach. The detection of genuine defects and separation of false alarms is achieved from the subtracted image [18]. This problem requires the renewed attention using purely computer vision approach, i.e. automated location of patterns using machine vision and detection of defects when the patterns are arbitrarily rotated and/or partially occluded. This approach is studied in present paper.

As will be shown, the properties of a composite material generate a specific class of mathematical models that can be used to optimize production and form controls in an automated control system (ACS) [1, 3]. Despite the high level of automation of technological processes in modern production, today there is a fairly high percentage of defects in production. Thus, the objective of the study required the solution of the following scientific problems [2, 5, 7, 9]:

- create an adequate control model of a composite material that can be used to automate the quality control of the material in all technological sites (steps) of production;

- solve the problem of identifying and assessing the quality of the composite material on the basis of an analysis of the real flow of events that occur during the quality control of the material;

- develop appropriate algorithms and methods for recognition of defects in composite materials on the basis of pattern recognition methods during identification of defects;

- solve the problem of creating technical means for quality control of textile production, which provide automation of the quality assessment process, with the development of appropriate methods and algorithms for their construction.

1. Generation of Reference Images

A reference image is generated, taking into account the results of preliminary analysis and a priori information about the object of control as a function of g , by compensating for external disturbances and comparing the image with the reference one to determine the phase shift. Next, the sample model is adjusted in accordance with the found phase shift - a comparison of the reference and the image, and the decision on the defectiveness of the fabric is made [4-8].

For modeling, let's choose a fabric of simple weave as the object of control. Since the fabric loses its ideal structure under the influence of external factors, it is necessary to model both the original ideal fabric and the skewed fabric, and also the defects that appear on its surface. Thus, to generate reference images, models of various types are needed:

- periodic models designed to describe periodic structures, such as fabrics modeled by Fourier series;

- aperiodic models designed to create models of local material defects using Kotelnikov time functions (wavelets);

- distributed models designed to describe defects that are distributed on the fabric, and for which the tensor apparatus is more suitable.

At the first stage of creating the model the object of control, the reference standard of the composite material fabric should be generated [5, 9-12]. Characteristic features necessary for the generation of the standard thread weave are:

- the radius of the threads, given by the style (type) of the material;

- the thread frequency - sets the density of the weave, which can be determined by preliminary Fourier analysis of the image.

For the formation of the ideal weave standard, we choose the following assumptions (Fig. 1):

- weft and warp threads are considered as round rods;
- cross-section of the threads remain unchanged after bending;
- the effect of crease is not taken into account;
- small corners;
- the bend of the thread is a sinusoid;
- weft and warp threads are equally bent with the same tensile strength.

These are common assumptions [6, 7, 14-16, 18] for standard types of weaves. Failure to comply with any of these assumptions should be taken into account by complicating the model.

With an arbitrary value of applied tensile forces on the weft and the warp, the picture is distorted. Moreover, if the weft tensile forces are directed at an angle to the perpendicular of the warp, then weft threads may be tilted by an angle, it is also should be taken into account in the model. Therefore, for a geometric model of interweaving, it is advisable to introduce correction parameters:

$$p_1 = \frac{F_0 - F_y \cdot \cos \alpha}{F_0 + F_y \cdot \cos \alpha}, \quad p_2 = \frac{F_y \cdot \cos \alpha - F_0}{F_0 + F_y \cdot \cos \alpha}, \quad (1)$$

where α – skew angle of weft threads.

With regard to the assumptions, the surface of the warp thread with the number is explicitly described by equations (A.2):

$$\begin{cases} (y - y_{oc_k})^2 + (z - z_{oc_k})^2 = r^2, \\ z_{oc_k} = r \cdot (1 + p_1) \cdot \cos(\omega_o(x - x_{yc_k})), \\ y_{oc_k} = y_{oc_1} + b \cdot (k - 1), \\ x_{yc_k} = x_{yc_1} + a \cdot (k - 1) + y_{oc_k} \cdot \operatorname{tg} \alpha. \end{cases} \quad (2)$$

The surface of the weft thread with a number is given by equations (A.3):

$$\begin{cases} (x - x_{yc_n})^2 + (z - z_{yc_n})^2 = r^2, \\ z_{yc_n} = r \cdot (1 + p_2) \cdot \cos(\omega_y(y - y_{oc_n})), \\ y_{oc_n} = y_{oc_1} + b \cdot (n - 1), \\ x_{yc_n} = x_{yc_1} + a \cdot (n - 1) + y \cdot \operatorname{tg} \alpha. \end{cases} \quad (3)$$

The use of corrective parameters allows obtaining a universal algorithm for generating a geometric

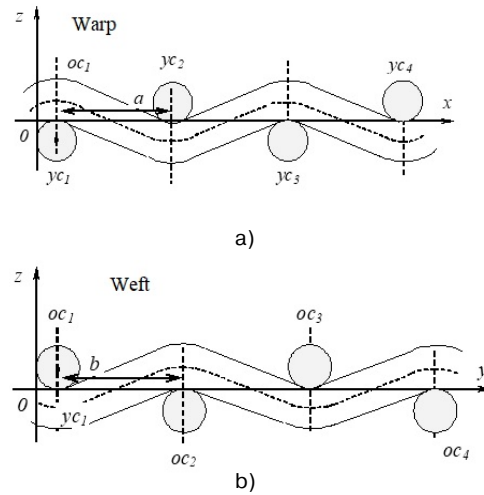


Fig. 1. The arrangement of fibers in the equilibrium state
a) warp threads, b) weft threads

model of interweaving for arbitrary tensile forces on weft and warp from 0 to F_{max} .

$$x = f_1(u, v), \quad y = f_2(u, v), \quad z = f_3(u, v). \quad (4)$$

To generate a reference image of a given size, the number of warp threads and the number of weft threads are ideally calculated, the coefficients and the corresponding tolerances are set. The image of each weft and warp thread is formed by equations (1) – (3). These equations have no explicit solution, and their parametric representation is used to build the thread surfaces. Fig. 2 shows the results of image generation by the developed algorithm for various values of characteristic parameters.

The speed of the automatic quality control system, in particular, the recognition system, can be increased through the use of a knowledge base on the basis of the generated samples, since the size of the library of reference images in this case turns out to be much less than the amount of memory needed to store all the reference images. The developed approach allows generating a mathematical description of the reference image, taking into account the mechanical characteristics of the composite material. Correction of the reference image created using periodic functions consists of adding defect models. To model local defects, it is advisable to use the wavelet apparatus, and for distributed defects, it is necessary to model the presence of tension in the node, turns, etc., which also allows comparing the weaving state with the reference image [4, 9, 17].

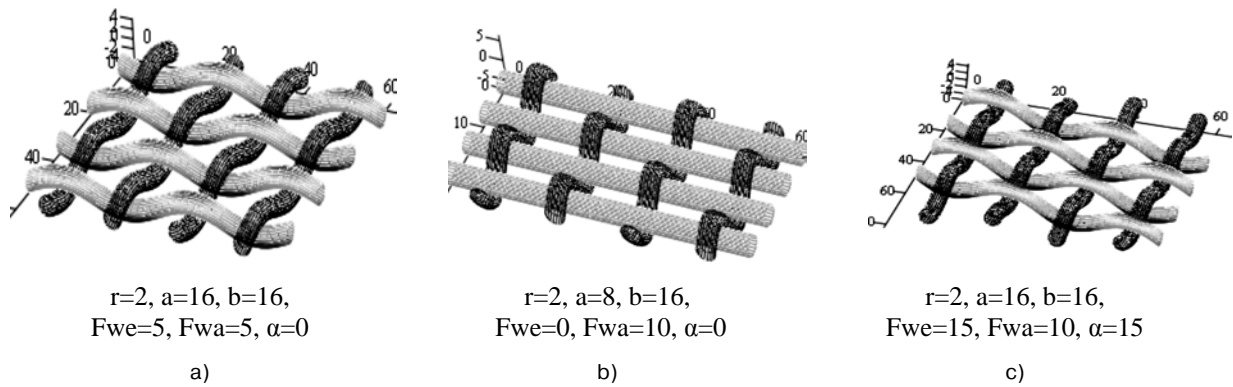


Fig. 2. The results of modeling reference images by the described method

The description of the interaction of the sensor and the object of control, in the case of using a frequency image, comes down to multiplying the spectral characteristic of the sensor window by the spectral characteristic of the object of control. However, the essential features of the mathematical description of composite materials and, in particular, textile fabrics as a test object impose their own characteristics on the mathematical model of the interaction of the inspected sample and sensor. Let us determine the response of the “object-sensor” system for a rolling window in the case of control of the material in the optical range (Fig. 3).

In this case, the reaction $U(x, y)$ is determined by the convolution (A.1) of the weighting weaving function $f(x, y)$ and the sensitivity distribution function of the sensor $H(x, y)$:

Let us consider the formation of the reaction of the optical sensor in the control of the material described by the model $f(x, y)$. Due to the mismatch between the definition area of the model and the window, the possibility of using convolution in the form (A.2) is lost.

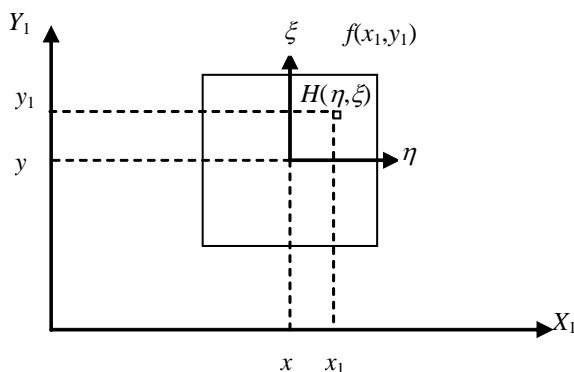


Fig. 3. Coordinate system for rolling window

Indeed, the measurement of coordinates of the model and the sensor window do not coincide, which leads to a violation of the convolution symmetry. This feature is almost ignored in modern studies. Actually, this property is inherent in the description of television systems. In this case, to change the variables, it is advisable to move to the X, Y coordinate system and the moving system η, ξ . As a result, the rolling window signal is described by the equation (A.3).

Introducing the model of weaving in the form of a Fourier series into the response equation, we get (A.4). Applying the transformation, we distinguish the spectral characteristic (5) of the sensor.

From the equations of the spectral matrix elements, we can distinguish the components associated with the moving coordinate system, which, in turn, will make it possible to obtain explicitly the components of the spectral characteristic of the sensor. Indeed, after grouping factors with moving coordinates and using the properties of operator linearity, we obtain an expression to determine the response of the system (A.10).

Designating elements associated with sensor characteristics as components relating to the corresponding elements of the spectral matrix of the fabric model, we obtain:

$$\begin{aligned}
 h^a_{m,n} &= \iint_{\Omega_H} H(\eta, \xi) \cos n\eta \cos m\xi d\eta d\xi, \\
 h^b_{m,n} &= \iint_{\Omega_H} H(\eta, \xi) \sin n\eta \cos m\xi d\eta d\xi, \\
 h^c_{m,n} &= \iint_{\Omega_H} H(\eta, \xi) \cos n\eta \sin m\xi d\eta d\xi \\
 h^d_{m,n} &= \iint_{\Omega_H} H(\eta, \xi) \sin n\eta \sin m\xi d\eta d\xi
 \end{aligned}
 \tag{5}$$

Substituting into [4-7] greatly simplifies the model of the system response. In expression (A.8), all elements of the weave model interact with the elements of the sensor model, which makes it expedient to move to a higher dimension space. To do this, we introduce vectors (A.9) with components of the spectral characteristics of the sensor h and the material a .

To describe the interaction, we introduce matrices that describe the sequence of interaction between the elements of the sensor model and the material (A.10). It is important that the resulting matrices are essentially cellular, the elements of which are the “tensile-compression” matrices and the rotation matrices (A.11). In this case, the matrix of the model of interaction between the sensor and the material has the form (A.12).

In the first place, the resulting model differs from the existing ones in that it allows saving the shape of the response image as a result of the interaction of two main elements of the material and the sensor model in the form (A.13).

In addition, the description of the control of the fabric of a deformed material is considerably simplified. Indeed, due to the fact that expression (A.10) has a simple core, the introduction of a deformed weave model comes down to simple operations on matrices. Using the matrices of the deformed weave model and the vectors of the excited model (A.11) allows determining the response of the “object-sensor” system (A.16) with the help of the spectral matrices (A.14) and (A.15).

Next, the sensor signal is generally described by the equation (A.16). Thus, a simple model was obtained that allows describing the structural properties of the composite material. On the other hand, spectral vectors can be written as the sum of the eigenvectors and conjugate vectors (A.17).

Thus, the evaluation of the components of spectral vectors cannot be done separately using a single sensor. Considering the actual capabilities of scanning systems that are used to control the quality of composite materials, we consider two main cases - scanning with the probe beam and using television sensors.

In the first case, the scanning (A.18) is performed by an element with a Gaussian energy distribution and an effective radius σ . The components of the spectral matrix of the decomposing

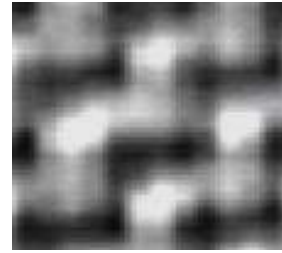


Fig. 4. The image of a test sample

element have the form (A.19), and therefore, the spectral matrix consists of elements (A.24). In this case, the spectral characteristic of the sensor provides filtering of the upper spatial frequencies without making significant distortion in the control signal. When using modern scanning methods using television cameras, the image of a scanning element in the form of a rectangle with uniform sensitivity is typical (Fig. 4).

The elements of the spectral matrix with the use of television sensors have the form (A.21). Probably, in this case, the influence of the geometric dimensions of the decomposing element of the control signal is more complex, which leads to a loss of sensitivity, as well as maxima of sensitivity to elements of the material structure. On the other hand, expression (A.21) determines a coefficient depending on the parameters of the decomposing element (A.22).

When building a model, it is necessary to take into account that preserving the explicit form of topological dependence ensures the unity of the approach to the identification of deviations in the quality of the material from the previously specified ones. In this case, to obtain a mathematical description, we use the complex form of a member of the series, where the partial sum of the series can be written in the form (A.23).

Considering the fact that in this expression we have samples over the lattice points with a shift along the coordinates by $3/2\pi$, we can write down (A.24). Thus, it is possible to obtain a description of the material while preserving the topological properties for shifts consistent with the geometric dimensions of the report. Returning to the control problem with a small rectangular window, we obtain a convolution (A.25). Taking into account that the sample is inscribed in a rectangle, for uniform sensitivity of the transducer in the window, we can write (A.26). So, the scanning

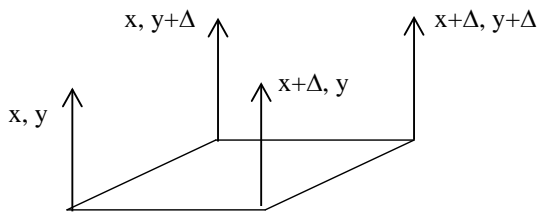


Fig. 5. Coordinates of function sampling

signal is formed of four components representing the Kotelnikov series. Samples are taken at points (x, y) , $(x + \Delta, y)$, $(x, y + \Delta)$, $(x + \Delta, y + \Delta)$ (Fig. 5).

Thus, the preservation of the sensitivity of the model to the topological properties of the sample is achieved by controlling the signal at its four points. Actually, given the fact that the spectrum of the fabric signal is limited, it can be argued that using (A.26) as a model provides the ability to reproduce the signal. On the other hand, it is possible to make an important conclusion - to control the quality of the composite material without losing information about the structural features, it is enough to have a 2×2 window that is comparable to the sample size (Fig. 6).

$f(x, y + \Delta)$	$f(x + \Delta, y + \Delta)$
$f(x, y)$	$f(x + \Delta, y)$

Fig. 6. The minimum size of the scan window in the absence of fabric deformation

$f(x, y + \Delta)$	$f(x + \Delta, y + \Delta)$
$f(x, y)$	$f(x + \Delta, y)$
$f(x, y - \Delta)$	$f(x + \Delta, y - \Delta)$

Fig. 7. The structure of the scan window while controlling the deformed weave

It is worth noticing that the presence of disturbances associated with the deformation of the material causes complications of the original model in the form of (A.16), and, as a result, two windows are required for control. However, in this case, the deformation matrix B is not predetermined. Therefore, it is impossible to determine the exact window configuration, and it remains to use the symmetry of the model (20) and the properties of the spectral vectors (A.17).

It follows from the analysis of equation (A.16) that only four components of spectral vectors are linearly independent. To control the fabric, in general, it is necessary to have a fairly simple window supplemented by delay components (Fig. 7).

Another important point is the need to determine the initial step in the window. This question is solved simply, if we consider that only the first harmonic is of interest in the control. So, the samples are taken at the points of maxima and zeros of the function. This statement is illustrated for the first harmonic in Fig. 8.

Thus, it is sufficient to simply build a model that preserves the main topological properties of

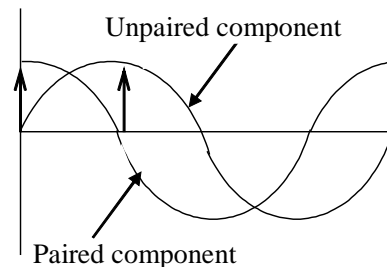


Fig. 8. Definition of paired and unpaired components

the material as an object of control according to the maxima of the function and its derivatives. Analyzing the resulting model, we can draw the following conclusions:

- a mathematical model of the interaction of fabric and the sensor is a sum of two rows;
- components of spectral vectors are determined only in the absence of deformation of the fabric structure;
- in the tasks of controlling the local fabric structure, it is possible to represent a mathematical model in the form of the Kotelnikov series;
- to preserve the topological properties of the weave in the model, the samples must be performed at the maxima of the function and its derivatives.

Composite fabric is a complex object of control, its description when interacting with the sensor and taking into account possible disturbances demonstrates the occurrence of a number of effects that can cause a decrease in the accuracy of control. The adequacy of the obtained mathematical description of the object of control and the phenomena arising in the process of control are not obvious and require careful verification.

2. Properties of Composite Fabrics as an Object of Control, Identified in the Course of Experimental Studies

The main feature of the studied materials is a certain frequency of repetition of the interweaving of the threads with respect to the simple structure of the fabric itself. Fig. 9 shows the image of some fabric samples with characteristic defects, obtained by scanning fabrics in the optical range [3-7].

The above mentioned samples of defects do not exhaust the entire spectrum of possible violations of the quality of the fabric, but these are the most difficult to detect types of defects.

Based on the theoretical assumptions and experimental data, we use the first harmonics of the Fourier series as the working model:

$$U(x, y) = U_0 + \sum_{i=1}^n U_{xi} \cos(\omega_{xi} x) + \sum_{j=1}^m U_{yj} \cos(\omega_{yj} y). \quad (6)$$

Considering the fact that the system must make a scanning motion to control the entire fabric web, we introduce the displacement speed of the scanning element along the coordinates V_x, V_y and the

speed of displacement of the fabric web V_T . Then, taking into account the linear dimensions of the sample, we obtain a model for the extremely small size of the scanning spot:

$$U(t) = U_0 + \sum_{i=1}^n U_{xi} \cos\left(\frac{2\pi}{l_x} V_x t\right) + \sum_{j=1}^m U_{yj} \cos\left(\frac{2\pi}{l_x} (V_y + V_T) t\right). \quad (7)$$

The resulting ratio is a weighting function and allows describing the actually expected signals with the introduction of the weighting function of the scanning element $h_s(x, y)$. Transforming the weighting function of the window with the response of the material, taking into account the moving coordinates, we obtain:

$$U(t) = U_0 S + \iint_S \left\{ h(x + V_x t, y + V_y t + V_T t) \left(\sum_{i=1}^n U_{xi} \cos\left(\frac{2\pi}{l_x} x\right) + \sum_{j=1}^m U_{yj} \cos\left(\frac{2\pi}{l_x} (y)\right) \right) \right\} dx dy. \quad (8)$$

With this representation, we obtain a fairly simple mathematical model of the scanning signal.

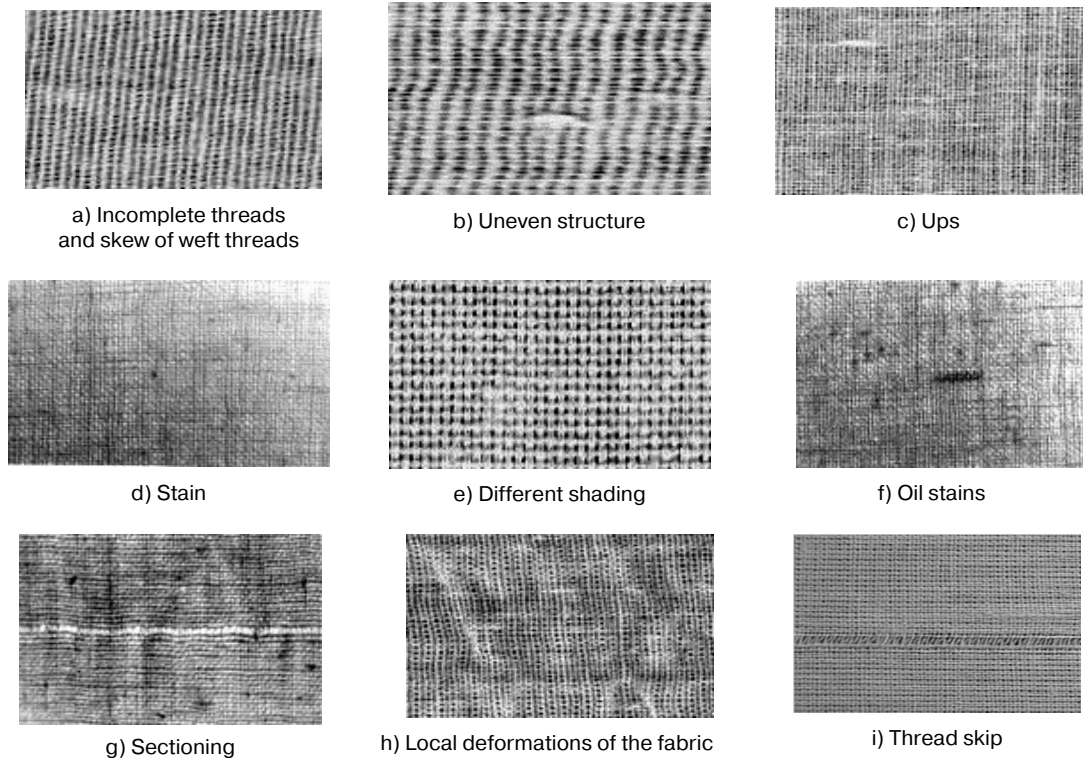


Fig. 9. Samples of textile fabric defects

However, it is necessary to take into account that the function of the scanning element window depends not only on the coordinates but also on the spectrum of the optical signal as follows:

$$U(t) = U_0 S + \iint_S \left\{ h(x + V_x t, y + V_y t + V_T t, \lambda) \left(\sum_{i=1}^n U_{xi}(\lambda) \cos\left(\frac{2\pi}{l_x} x\right) + \sum_{j=1}^m U_{yj}(\lambda) \cos\left(\frac{2\pi}{l_x} y\right) \right) \right\} dx dy \tag{9}$$

The obtained description of the scanning signal allows us to represent it as a combination of three processes - scanning the backing layer, the warp threads system, and the weft threads system. Thus, it is advisable to limit the mathematical weave model to the following components:

- mathematical expectation of the fabric structure described as a weighting function (6) with the dependences of the coefficients on the skew of the fabric elements;

- convolution of the weighting function of the sample and the characteristics of the decomposing element (7);

- random field $U_0(x, y)$ associated with uneven fabric web and scanning noise.

Thus, the canonical image of a random process was chosen as the working theoretical model, where the role of the mathematical expectation is played by the first harmonic of the binary image of the fabric web structure, and the elementary functions have a Fourier basis. With this representation, it becomes possible to obtain a description of defects in the sample structure as a Fourier image of the generating binary function.

The study of the process of defect identification.

On the scanner mock-up, the study of signals for scanning composite fabric defects was performed. The results for the main types of fabric defects obtained during the experiment are given in Table 1 –Table 5 and in Fig. 10 – Fig. 14 (U(B) is scanner output, n – corresponds to defects in the fabric elements).

Table 1. Results according to the distribution of the signal at the defect "Oil stains"

U (B)	-1.2	-1.125	-1.05	-0.975	-0.9	-0.825	-0.75	-0.675	-0.6
n	3	8	28	29	0	28	5	4	3

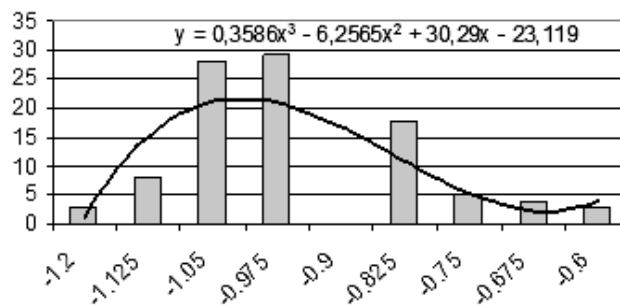


Fig. 10. Signal distribution at the defect "Oil stains"

Table 2. Data on the distribution of the signal at the defect "Seam"

U (Y)	-2.3	-2.2	-2.1	-2	-1.9	-1.8	-1.7	-1.6	-1.5
n	7	10	25	10	15	11	7	3	1

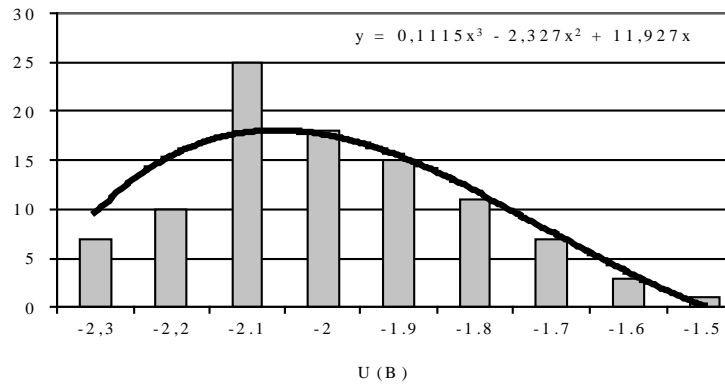


Fig. 11. Data on the distribution of the signal at the defect "Seam"

Table 3. Data on the distribution of the signal at the defect "Stains"

U (B)	-1.5	-1.125	-1.35	-1.275	-1.125	-1.05	-0.75	-0.975	-0.9
n	1	6	21	0	30	21	15	7	3

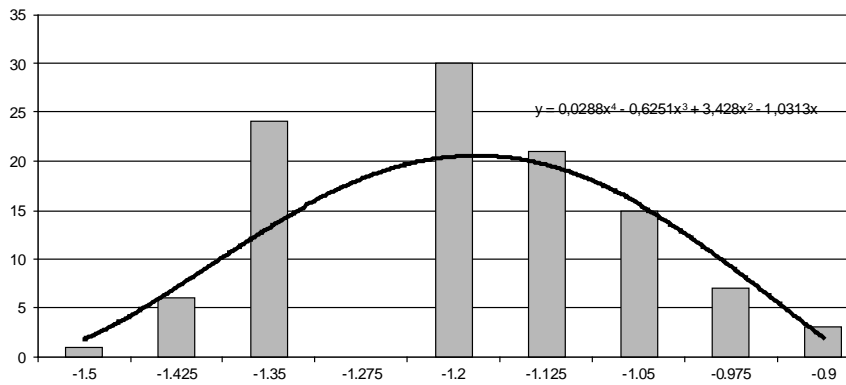


Fig. 12. Data on the distribution of the signal at the defect "Stains"

Table 4. Data on the distribution of the signal at the defect "Holes"

U (B)	1	2.969	3.1	3.41	3.63	3.8	4.1	4.28
n	4	10	15	16	22	16	9	5

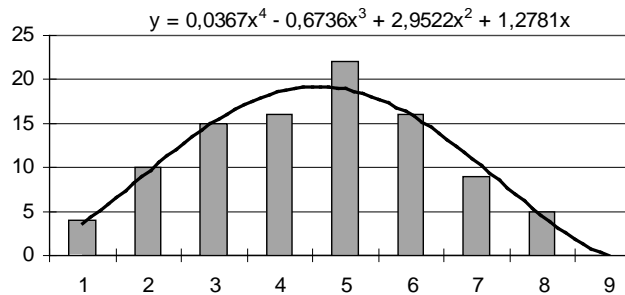


Fig. 13. Data on the distribution of the signal at the defect "Holes"

Table 5. Data on the distribution of the signal at the defect "Sectioning"

U (B)	1.5	1.75	2	2.25	2.5	2.75	3	3.25
n	4	12	23	33	33	20	5	1

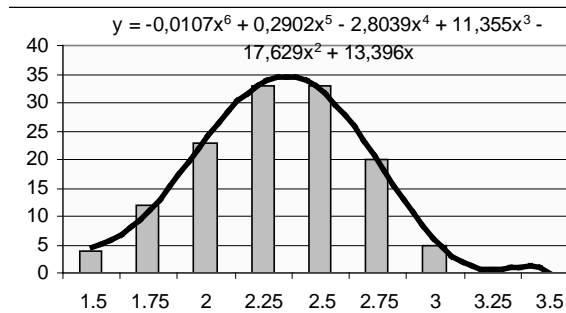


Fig. 14. Data on the distribution of the signal at the defect "Sectioning"

As can be seen from the experimental results, the defect signals have statistically stable interfaces. At the same time, it is necessary to take into account the entire ensemble, including the distribution characteristic of fabrics without defects. Based on the assumption of using a mathematical model of fabric in describing the processes of automated quality control of fabric using the optical system, it is important to determine the effect of system parameters on the quality of control. The analysis of a mathematical model of a fabric shows the presence of a multiplier that relates the amplitudes of the harmonics to the geometric dimensions of the scanning window. Consequently, when building a laser scanner to detect fabric defects, there is a real possibility of confidently separating signals from defective areas.

Thus, a model of dependence of the control signals on the size of the sensor window appears:

$$U(l, h) = U_0 + U_{lh} \frac{\sin(2\pi l / L) \sin(2\pi h / H)}{2\pi l / L \cdot 2\pi h / H}, \quad (10)$$

where U_0 – the value of the average response; U_{lh} – the value of the maximum error; l – the size of the window in the direction of the weft; h – the size of the window in the direction of the warp; L – the maximum size of the window in the direction of the weft; H – the maximum size of the window in the direction of the warp.

To determine the adequacy of this model of the influence of the window size, an experiment was conducted, in which the window size changed in the direction of the weft. In this case, a response dependency was expected in the form:

$$U(l, h) = U_0 + U_{lh} \frac{\sin(2\pi l / L)}{2\pi l / L}. \quad (11)$$

Fig. 15 shows the polygon of the amplitude distribution of the signals of fabric defects without taking into account the sign of the defect and taking into account the sign of the defect detection signal, which was obtained using the computer vision system.

The computer vision system included optical sensors, implemented an algorithm for processing its output according to the equations described above. As a result, the series of experiments on the detection of defects on test tissue samples, signal amplitude distributions were constructed depending on the nature of the defect. The diagrams show the analysis of the distributions, taking into account the sign of the defect detector signal, allows us to classify almost all types of defects considered. For example, using artificial neural networks and more classic, deterministic methods. Certain difficulties arise in the determination of defects such as "strain" and "falling of threads".

Preliminary experiments have shown that the model is effective when used in conjunction with a direct propagation neural network and the support vector method.

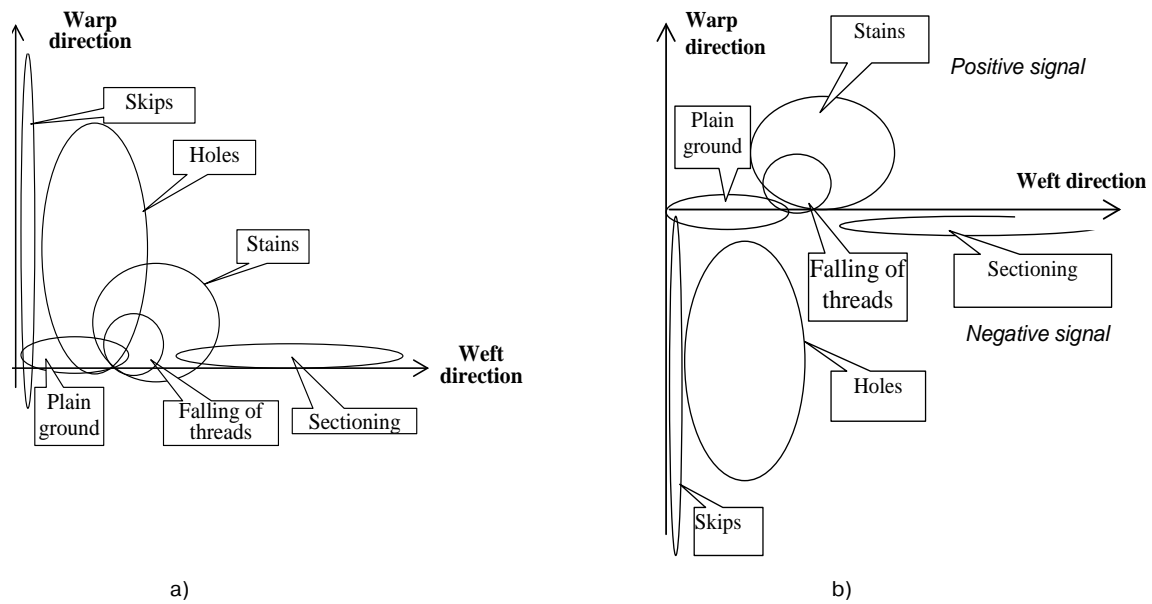


Fig. 15. Distribution of amplitudes of signals of fabric defects (space m)

a) without taking into account the sign of the defect b) taking into account the sign of the defect detection signal

Conclusion

The goal of the study is the development of methods for the automatic inspection of composite materials in production using optical sensors and computer vision systems. To achieve the goal, the following scientific problems were solved: the model of the composite material adequate to the task of control was created, which can be used to automate the quality control of the material at all technological sites (steps) of production; the problem of identifying and assessing the quality of the composite material was solved on the basis of the

analysis of the real flow of events occurring during the quality control of the material; appropriate algorithms and methods for recognition of defects in composite materials based on pattern recognition methods for identifying defects are developed.

The method for generating mathematical models of reference fabric samples and the method for comparing images of physical samples of composite materials with them are proposed. The high efficiency of application of the proposed methods in conjunction with defect classification systems, for example, using artificial neural networks, can be shown.

Appendix A

The reaction:

$$U(x, y) = \iint_{\Omega_H} f(x_1, y_1) H(x_1 - x, y_1 - y) dx_1 dy_1 . \quad (\text{A.1})$$

The possibility of using convolution is lost in the following form:

$$U(x, y) = \iint_{\Omega_H} f(x_1 - x, y_1 - y) H(x_1, y_1) dx_1 dy_1 . \quad (\text{A.2})$$

The rolling window signal is described by the equation:

$$U(x, y) = \iint_{\Omega_H} f(\eta + x, \xi + y)H(\eta, \xi)d\eta d\xi . \tag{A.3}$$

$$\begin{aligned} U(x, y) &= \tilde{f}(x, y) \otimes H(x, y) = \iint_{\Omega_H} \tilde{f}(\eta + x, \xi + y)H(\eta, \xi)d\eta d\xi = \\ &= \iint_{\Omega_H} H(\eta, \xi) \left[\sum_{m=0}^{\infty} \sum_{n=0}^{\infty} \lambda_{m,n} (a_{m,n} \cos n(\eta + x) \cos m(\xi + y) + \dots \right. \\ &\quad \left. + b_{m,n} \sin n(\eta + x) \cos m(\xi + y) + c_{m,n} \cos n(\eta + x) \sin m(\xi + y) + \dots \right. \\ &\quad \left. + d_{m,n} \sin n(\eta + x) \sin m(\xi + y)) \right] d\eta d\xi. \end{aligned} \tag{A.4}$$

Spectral characteristic of the sensor:

$$\begin{aligned} \tilde{f}(x, y) &= \iint_{\Omega_H} H(\eta, \xi) \left[\sum_{m=0}^{\infty} \sum_{n=0}^{\infty} \lambda_{m,n} (a_{m,n} \cos n(\eta + x) \cos m(\xi + y) + \right. \\ &\quad \left. + b_{m,n} \sin n(\eta + x) \cos m(\xi + y) + c_{m,n} \cos n(\eta + x) \sin m(\xi + y) + \right. \\ &\quad \left. + d_{m,n} \sin n(\eta + x) \sin m(\xi + y)) \right] d\eta d\xi; \end{aligned} \tag{A.5}$$

where

$$\begin{aligned} a_{m,n} \cos n(\eta + x) \cos m(\xi + y) &= a_{m,n} [(\cos n\eta \cos nx - \sin n\eta \sin nx) \times \\ &\times (\cos m\xi \cos my - \sin m\xi \sin my)] = \\ &= a_{m,n} [\cos n\eta \cos nx \cos m\xi \cos my - \sin n\eta \sin nx \cos m\xi \cos my - \\ &- \cos n\eta \cos nx \sin m\xi \sin my + \sin n\eta \sin nx \sin m\xi \sin my]; \end{aligned}$$

$$\begin{aligned} b_{m,n} \sin n(\eta + x) \cos m(\xi + y) &= b_{m,n} [(\sin n\eta \cos nx + \cos n\eta \sin nx) \times \\ &(\cos n\eta \cos nx - \sin n\eta \sin nx)] = \\ &= b_{m,n} [\sin n\eta \cos nx \cos m\xi \cos my + \cos n\eta \sin nx \cos m\xi \cos my - \\ &- \sin n\eta \cos nx \sin m\xi \sin my - \cos n\eta \sin nx \sin m\xi \sin my]; \end{aligned}$$

$$\begin{aligned} c_{m,n} \cos n(\eta + x) \sin m(\xi + y) &= c_{m,n} [(\cos n\eta \cos nx - \sin n\eta \sin nx) \times \\ &\times (\sin m\xi \cos my + \cos m\xi \sin my)] = \\ &= c_{m,n} [\cos n\eta \cos nx \sin m\xi \cos my - \sin n\eta \sin nx \sin m\xi \cos my + \\ &+ \cos n\eta \cos nx \cos m\xi \sin my - \sin n\eta \sin nx \cos m\xi \sin my]; \end{aligned}$$

$$\begin{aligned} d_{m,n} \sin n(\eta + x) \sin m(\xi + y) &= d_{m,n} [(\sin n\eta \cos nx + \cos n\eta \sin nx) \times \\ &\times (\sin m\xi \cos my + \cos m\xi \sin my)] = \\ &= d_{m,n} [(\sin n\eta \cos nx \sin m\xi \cos my + \cos n\eta \sin nx \sin m\xi \cos my + \\ &+ \sin n\eta \cos nx \cos m\xi \sin my + \cos n\eta \sin nx \cos m\xi \sin my)]. \end{aligned}$$

The response of the system.

$$\begin{aligned}
 U(x, y) = & \sum_{m=0}^{\infty} \sum_{n=0}^{\infty} \lambda_{m,n} (a_{m,n} \{ [\iint_{\Omega_H} H(\eta, \xi) \cos n\eta \cos m\xi d\eta d\xi] \cos nx \cos my - \\
 & - [\iint_{\Omega_H} H(\eta, \xi) \sin n\eta \cos m\xi d\eta d\xi] \sin nx \cos my - \\
 & - [\iint_{\Omega_H} H(\eta, \xi) \cos n\eta \sin m\xi d\eta d\xi] \cos nx \sin my + \\
 & + [\iint_{\Omega_H} H(\eta, \xi) \sin n\eta \sin m\xi d\eta d\xi] \sin nx \sin my \} + \\
 & + b_{m,n} \{ [\iint_{\Omega_H} H(\eta, \xi) \sin n\eta \cos m\xi d\eta d\xi] \cos nx \cos my + \\
 & + [\iint_{\Omega_H} H(\eta, \xi) \cos n\eta \cos m\xi d\eta d\xi] \sin nx \cos my - \\
 & - [\iint_{\Omega_H} H(\eta, \xi) \sin n\eta \sin m\xi d\eta d\xi] \cos nx \sin my - \\
 & - [\iint_{\Omega_H} H(\eta, \xi) \cos n\eta \sin m\xi d\eta d\xi] \sin nx \sin my \} + \\
 & + c_{m,n} \{ [\iint_{\Omega_H} H(\eta, \xi) \cos n\eta \sin m\xi d\eta d\xi] \cos nx \cos my - \\
 & - [\iint_{\Omega_H} H(\eta, \xi) \sin n\eta \sin m\xi d\eta d\xi] \sin nx \cos my + \\
 & + [\iint_{\Omega_H} H(\eta, \xi) \cos n\eta \cos m\xi d\eta d\xi] \cos nx \sin my - \\
 & - [\iint_{\Omega_H} H(\eta, \xi) \sin n\eta \cos m\xi d\eta d\xi] \sin nx \sin my \} + \\
 & + d_{m,n} \{ [\iint_{\Omega_H} H(\eta, \xi) \sin n\eta \sin m\xi d\eta d\xi] \cos nx \cos my + \\
 & + [\iint_{\Omega_H} H(\eta, \xi) \cos n\eta \sin m\xi d\eta d\xi] \sin nx \cos my + \\
 & + [\iint_{\Omega_H} H(\eta, \xi) \sin n\eta \cos m\xi d\eta d\xi] \cos nx \sin my + \\
 & + [\iint_{\Omega_H} H(\eta, \xi) \cos n\eta \cos m\xi d\eta d\xi] \sin nx \sin my \} \}.
 \end{aligned} \tag{A.6}$$

Designating elements associated with sensor characteristics as components relating to the corresponding elements of the spectral matrix of the fabric model, we obtain:

$$\begin{aligned}
 h^a_{m,n} &= \iint_{\Omega_H} H(\eta, \xi) \cos n\eta \cos m\xi d\eta d\xi, \\
 h^b_{m,n} &= \iint_{\Omega_H} H(\eta, \xi) \sin n\eta \cos m\xi d\eta d\xi, \\
 h^c_{m,n} &= \iint_{\Omega_H} H(\eta, \xi) \cos n\eta \sin m\xi d\eta d\xi, \\
 h^d_{m,n} &= \iint_{\Omega_H} H(\eta, \xi) \sin n\eta \sin m\xi d\eta d\xi.
 \end{aligned} \tag{A.7}$$

Simplifying the model of the system response:

$$\begin{aligned}
 U(x, y) = & \sum_{m=0}^{\infty} \sum_{n=0}^{\infty} \lambda_{m,n} (h^a_{m,n} a_{m,n} + h^b_{m,n} b_{m,n} + h^c_{m,n} c_{m,n} + h^d_{m,n} d_{m,n}) \cos nx \cos my + \\
 & + (-h^b_{m,n} a_{m,n} + h^a_{m,n} b_{m,n} - h^d_{m,n} c_{m,n} + h^c_{m,n} d_{m,n}) \sin nx \cos my + \\
 & + (-h^c_{m,n} a_{m,n} - h^d_{m,n} b_{m,n} + h^a_{m,n} c_{m,n} + h^b_{m,n} d_{m,n}) \cos nx \sin my + \\
 & + (h^d_{m,n} a_{m,n} - h^c_{m,n} b_{m,n} - h^b_{m,n} c_{m,n} + h^a_{m,n} d_{m,n}) \sin nx \sin my.
 \end{aligned} \tag{A.8}$$

Vectors with components of the spectral characteristics of the sensor h and the material a :

$$\mathbf{h}_{m,n} = \begin{bmatrix} h^a_{m,n} \\ h^b_{m,n} \\ h^c_{m,n} \\ h^d_{m,n} \end{bmatrix}, \quad \mathbf{a}_{m,n} = \begin{bmatrix} a_{m,n} \\ b_{m,n} \\ c_{m,n} \\ d_{m,n} \end{bmatrix}. \tag{A.9}$$

We introduce matrices that describe the sequence of interaction between the elements of the sensor model and the material:

$$\begin{aligned}
 M_a = \begin{pmatrix} 1 & 0 & 0 & 0 \\ 0 & 1 & 0 & 0 \\ 0 & 0 & 1 & 0 \\ 0 & 0 & 0 & 1 \end{pmatrix}, \quad M_b = \begin{pmatrix} 0 & -1 & 0 & 0 \\ 1 & 0 & 0 & 0 \\ 0 & 0 & 0 & -1 \\ 0 & 0 & 1 & 0 \end{pmatrix}, \\
 M_c = \begin{pmatrix} 0 & 0 & -1 & 0 \\ 0 & 0 & 0 & -1 \\ 1 & 0 & 0 & 0 \\ 0 & 1 & 0 & 0 \end{pmatrix}, \quad M_d = \begin{pmatrix} 0 & 0 & 0 & 1 \\ 0 & 0 & -1 & 0 \\ 0 & -1 & 0 & 0 \\ 1 & 0 & 0 & 0 \end{pmatrix}.
 \end{aligned} \tag{A.10}$$

The rotation matrices:

$$F(X1, X2) \tag{A.11}$$

The matrix of the model of interaction between the sensor and the material has the form:

$$S^u_{m,n} = \begin{pmatrix} \mathbf{a}_{m,n} M_a \mathbf{h}_{m,n} & \mathbf{a}_{m,n} M_b \mathbf{h}_{m,n} \\ \mathbf{a}_{m,n} M_c \mathbf{h}_{m,n} & \mathbf{a}_{m,n} M_d \mathbf{h}_{m,n} \end{pmatrix}. \tag{A.12}$$

The sensor model in the form:

$$U(x, y) = \sum_{m=0}^{\infty} \sum_{n=0}^{\infty} \lambda_{m,n} \langle \vec{\phi}_{mx}, S^u_{m,n} \vec{\phi}_{ny} \rangle. \tag{A.13}$$

The spectral matrices:

$$\mathbf{a}^+_{m,n} = \begin{bmatrix} a^+_{m,n} \\ b^+_{m,n} \\ c^+_{m,n} \\ d^+_{m,n} \end{bmatrix}, \quad \mathbf{a}^-_{m,n} = \begin{bmatrix} a^-_{m,n} \\ b^-_{m,n} \\ c^-_{m,n} \\ d^-_{m,n} \end{bmatrix}. \tag{A.14}$$

$$\begin{aligned}
 S^{u+}_{m,n} &= \begin{pmatrix} \mathbf{a}^+_{m,n} M_a \mathbf{h}_{m,n} & \mathbf{a}^+_{m,n} M_b \mathbf{h}_{m,n} \\ \mathbf{a}^+_{m,n} M_c \mathbf{h}_{m,n} & \mathbf{a}^+_{m,n} M_d \mathbf{h}_{m,n} \end{pmatrix}, \\
 S^{u-}_{m,n} &= \begin{pmatrix} \mathbf{a}^-_{m,n} M_a \mathbf{h}_{m,n} & \mathbf{a}^-_{m,n} M_b \mathbf{h}_{m,n} \\ \mathbf{a}^-_{m,n} M_c \mathbf{h}_{m,n} & \mathbf{a}^-_{m,n} M_d \mathbf{h}_{m,n} \end{pmatrix}.
 \end{aligned} \tag{A.15}$$

The sensor signal is generally described by the equation:

$$U(x, y) = \sum_{m=0}^{\infty} \sum_{n=0}^{\infty} \lambda_{m,n} \langle \vec{\phi}_{nx}^+, S^{u+}_{m,n} \vec{\phi}_{my}^+ \rangle + \sum_{m=0}^{\infty} \sum_{n=0}^{\infty} \langle \lambda_{m,n}, \vec{\phi}_{mx}^- S^{u-}_{m,n} \vec{\phi}_{ny}^- \rangle. \quad (\text{A.16})$$

Spectral vectors can be written as the sum of the eigenvectors and conjugate vectors:

$$\mathbf{a}_{m,n}^+ = \frac{1}{2} \begin{bmatrix} a_{m,n}^+ + d_{m,n}^+ \\ b_{m,n}^+ + c_{m,n}^+ \\ c_{m,n}^+ + b_{m,n}^+ \\ d_{m,n}^+ + a_{m,n}^+ \end{bmatrix} = \mathbf{a}_{m,n}^+ + \tilde{\mathbf{a}}_{m,n}^+, \quad (\text{A.17})$$

$$\mathbf{a}_{m,n}^- = \frac{1}{2} \begin{bmatrix} a_{m,n}^- - d_{m,n}^- \\ b_{m,n}^- - c_{m,n}^- \\ c_{m,n}^- - b_{m,n}^- \\ d_{m,n}^- - a_{m,n}^- \end{bmatrix} = \mathbf{a}_{m,n}^- - \tilde{\mathbf{a}}_{m,n}^-,$$

The scanning is performed by an element with a Gaussian energy distribution and an effective radius σ :

$$\rho(x, y) = \exp(-\sigma^2(x^2 + y^2)). \quad (\text{A.18})$$

The components of the spectral matrix of the decomposing element have the form:

$$h_a = 1/2 \exp(-(m^2 + n^2)/4\sigma^2), \quad (\text{A.19})$$

and the spectral matrix consists of the following elements:

$$\begin{aligned} A_{mn} &= 1/2\pi a_{mn} \exp(-(m^2 + n^2)/4\sigma^2); \\ B_{mn} &= 1/2\pi b_{mn} \exp(-(m^2 + n^2)/4\sigma^2); \\ X_4 &= XS = \text{SIGN}Y \cdot (XY); \\ D_{mn} &= 1/2\pi d_{mn} \exp(-(m^2 + n^2)/4\sigma^2). \end{aligned} \quad (\text{A.20})$$

The elements of the spectral matrix with the use of television sensors have the form:

$$\begin{aligned} A_{mn} &= \frac{a_{mn}}{\pi^2} \frac{\sin(mL/2)}{mL/2} \frac{\sin(nh/2)}{nh/2}, \\ B_{mn} &= \frac{-b_{mn}}{\pi^2} \frac{\sin(mL/2)}{mL/2} \frac{\sin(nh/2)}{nh/2}, \\ C_{mn} &= \frac{-c_{mn}}{\pi^2} \frac{\sin(mL/2)}{mL/2} \frac{\sin(nh/2)}{nh/2}, \\ D_{mn} &= \frac{d_{mn}}{\pi^2} \frac{\sin(mL/2)}{mL/2} \frac{\sin(nh/2)}{nh/2}. \end{aligned} \quad (\text{A.21})$$

The parameters of the decomposing element:

$$\frac{\sin(mL/2)}{mL/2} \frac{\sin(nh/2)}{nh/2} = \text{sinc}(mL/2, nh/2). \quad (\text{A.22})$$

The partial sum of the series can be written in the form:

$$\begin{aligned} \tilde{f}_{mn}(x, y) &= a_{m,n} \cos nx \cos my + b_{m,n} \sin nx \cos my + \\ &+ c_{m,n} \cos nx \sin my + d_{m,n} \sin nx \sin my = \\ &= r_{m,n} e^{j(nx+my)} + r_{-m,n} e^{j(nx-my)} + r_{m,-n} e^{j(-nx+my)} + r_{-m,-n} e^{-j(nx+my)}. \end{aligned} \tag{A.23}$$

we can write down:

$$\begin{aligned} \tilde{f}(x, y) &= \sum_{m=0}^{\infty} \sum_{n=0}^{\infty} r_{m,n} e^{j(nx+my)} + \sum_{m=0}^{\infty} \sum_{n=0}^{\infty} r_{-m,n} e^{j(nx-my)} + \\ &+ \sum_{m=0}^{\infty} \sum_{n=0}^{\infty} r_{m,-n} e^{j(-nx+my)} + \sum_{m=0}^{\infty} \sum_{n=0}^{\infty} r_{-m,-n} e^{-j(nx+my)} = \\ &= f^*(x, y) + f^*(x, y + \Delta_y) + f^*(x + \Delta_x, y) + f^*(x + \Delta_x, y + \Delta_y). \end{aligned} \tag{A.24}$$

Returning to the control problem with a small rectangular window, we obtain a convolution:

$$\begin{aligned} U(x, y) &= H \otimes \{f^*(x, y) + f^*(x, y + \Delta_y) + \\ &+ f^*(x + \Delta_x, y) + f^*(x + \Delta_x, y + \Delta_y)\}. \end{aligned} \tag{A.25}$$

we can write:

$$\alpha \tag{A.26}$$

References

1. Drobina Robert, Machnio Mieczyslaw S. Application of the image analysis technique for textile identification AUTEK Research Journal. Vol. 6, № 1. 40 – 48
2. Farooq U., Tim King T., Gaskell P. H., Kapur N. A mechatronic approach for automatic inspection of deformable webs. University of Twente. Proc. of Mechatronics. 2002. 663 – 674.
3. Islam A., Akhter S., Mursalin T.E. Automated Textile Defect Recognition System Using Computer Vision and Artificial Neural Networks. ENFORMATIKA. – 2006. Vol.13. 1 – 6.
4. Kumar A. Inspection of surface defects using optimal FIR filters. Proc. ICASSP-2003, Hong Kong, Apr. 2003. Vol.3. Is.2. 241 – 244. <http://www4.comp.polyu.edu.hk/~csajaykr/myhome/publication.htm>
5. Kumar A., Shen Helen C. Texture inspection for defects using neural networks and support vector machines. IEEE ICIP. – 2002. Vol.III 353 – 356.
6. Rong Fu, Meihong Shi, Hongli Wei, and Huijuan Chen. Fabric Defect Detection Based on Adaptive Local Binary Patterns. Proceedings of the 2009 IEEE. International Conference on Robotics and Biomimet. December 19 -23, 2009, Guilin, China. 1336-1340.
7. Mak K. L., Peng P. Detecting Defects in Textile Fabrics with Optimal Gabor Filters//ENFORMATIKA. – 2006. Vol.13. 75 – 80.
8. Postle Jacqueline R., Postle R. Modelling fabric deformation as a nonlinear dynamical system using Bäcklund Transformations. International Journal of Clothing Science and Technology. 1996. Vol. 8. Is. 3. 22 – 42.
9. Prinya T. Machine Vision for Quality Inspection of Cotton in the Textile Industry. Thammasat Int. J. Sc. Tech., Vol.6, № 1. 60 – 63.
10. United States Patent 6,753,965 B2; Current International Class: G01N 21/88 (20060101); G01N 21/898 (20060101); G01N 021/84; G01N 021/00. Defect detection system for quality assurance using automated visual inspection / Kumar; Ajay (Kanpur, IN), Pang; Kwok-Hung Grantham (Hong Kong, CN). Data of Patent: June 22, 2004.
11. Valiente1 José M., Carmen Carretero M.; Gómis José M.; Albert F. Image Processing Tool for the Purpose of Textile Fabric Modeling// XII ADM International Conference. – Rimini, Italy. 7, 2001. G1. – P.56 – 64.
12. Rozhkov S.O., Ternova T.I., Hodinovich M.B. Problems of the manifestation of the development of tissue defects in the process of discolouration. Prazi syomoi all-ukrainian mizhdivnirochni conferenceii UkrObraz'2004. Sampling signal and image and recognition. 151 - 154.
13. Rozhkov S.O., Brazhnik D.O. Victory of neuromoregular structures for stimulating recognition systems with compensation for information flows. Praxis of the All-Ukrainian International Conference UkrObraz'2004 Sampling signal and image recognition. 37 - 40.

14. Zhilenkov A., Chernyi S. Investigation Performance of Marine Equipment with Specialized Information Technology. *Procedia Engineering*, 100 (2015), 1247-1252. doi: 10.1016/j.proeng.2015.01.490
15. Nyrkov A., Zhilenkov A., Sokolov S. and Chernyi S. (2018) "Hard- and Software Implementation of Emergency Prevention System for Maritime Transport" *Automation and Remote Control* 79:1 195-202. DOI: 10.1134/S0005117918010174
16. Sokolov, S.; Zhilenkov, A.; Chernyi, S.; Nyrkov, A.; Mamunts, D. Dynamics Models of Synchronized Piecewise Linear Discrete Chaotic Systems of High Order. *Symmetry* 2019, 11, 236, doi:10.3390/sym11020236.
17. Zhilenkov, A.; Chernyi, S.; Sokolov, S.; Nyrkov, A. Intelligent autonomous navigation system for UAV in randomly changing environmental conditions. *J. Intell. Fuzzy Syst.* 2020, 1–7, doi:10.3233/jifs-179741
18. A. Kumar, "Computer-Vision-Based Fabric Defect Detection: A Survey," in *IEEE Transactions on Industrial Electronics*, vol. 55, no. 1, pp. 348-363, Jan. 2008, doi: 10.1109/TIE.1930.896476.

Zhilenkov A. A. St. Petersburg State Marine Technical University (SMTU), St. Petersburg, Russian Federation Head of the Department of Cyberphysical Systems, Cand. Sci. (Eng.), Assoc. Prof. Publications: 167 (3) Research interests: cyber-physical systems, automatic control, modeling, artificial intelligence, robotics. Email: zhilenkovanton@gmail.com

Chernyi S. G. Kerch State Maritime Technological University, 2983095, Russia, Kerch, Ordzonikidze st., 82. Head of the Department of Ship Electrical Equipment and Industrial Automation, PhD. Admiral Makarov State University of Maritime and Inland Shipping, 198035, Russia, Saint-Petersburg, Dvinskaya st., 5/7. Associate Professor, PhD, Associate Professor. Number of publications: 100 (including 3 monographs and 2 books). IEEE, DAAAM, EAI Membership. Member of the Editorial Board of MDPI, Hindawi journals. Research interests: information technology, modeling of heterogeneous systems. Email: sergiiblack@gmail.com